ABCB5-Mediated Doxorubicin Transport and Chemoresistance in Human Malignant Melanoma

Natasha Y. Frank,[1] Armen Margaryan,[2] Ying Huang,[3] Tobias Schatton,[2] Ana Maria Waaga-Gasser,[4] Martin Gasser,[4] Mohamed H. Sayegh,[2] Wolfgang Sadee,[3] and Markus H. Frank[2]

[1]Department of Genetics, Children's Hospital Boston and [2]Transplantation Research Center, Brigham and Women's Hospital and Children's Hospital Boston, Harvard Medical School, Boston, Massachusetts; [3]Program in Pharmacogenomics, Department of Pharmacology, The Ohio State University, Columbus, Ohio; and [4]Department of Surgery, University of Würzburg Medical School, Würzburg, Germany

Abstract

Enhanced drug efflux mediated by ABCB1 P-glycoprotein and related ATP-binding cassette transporters is one of several mechanisms of multidrug resistance thought to impair chemotherapeutic success in human cancers. In malignant melanoma, its potential contribution to chemoresistance is uncertain. Here, we show that ABCB5, which functions as a determinant of membrane potential and regulator of cell fusion in physiologic skin progenitor cells, is expressed in clinical malignant melanoma tumors and preferentially marks a subset of hyperpolarized, CD133$^+$ stem cell phenotype-expressing tumor cells in malignant melanoma cultures and clinical melanomas. We found that ABCB5 blockade significantly reversed resistance of G3361 melanoma cells to doxorubicin, an agent to which clinical melanomas have been found refractory, resulting in a 43% reduction in the LD_{50} from 4 to 2.3 μmol/L doxorubicin ($P < 0.05$). Our results identified ABCB5-mediated doxorubicin efflux transport as the underlying mechanism of resistance, because ABCB5 blockade significantly enhanced intracellular drug accumulation. Consistent with this novel ABCB5 function and mechanism in doxorubicin resistance, gene expression levels of the transporter across a panel of human cancer cell lines used by the National Cancer Institute for drug screening correlated significantly with tumor resistance to doxorubicin ($r = 0.44$; $P = 0.016$). Our results identify ABCB5 as a novel drug transporter and chemoresistance mediator in human malignant melanoma. Moreover, our findings show that ABCB5 is a novel molecular marker for a distinct subset of chemoresistant, stem cell phenotype-expressing tumor cells among melanoma bulk populations and indicate that these chemoresistant cells can be specifically targeted via ABCB5 to enhance cytotoxic efficacy. (Cancer Res 2005; 65(10): 4320-33)

Introduction

Cancer chemotherapeutic efficacy is frequently impaired by either intrinsic or acquired tumor resistance to multiple, structurally unrelated therapeutic drugs with different mechanisms of action, a phenomenon termed multidrug resistance (MDR; reviewed in ref. 1). MDR can result from several distinct mechanisms, including alterations of tumor cell cycle checkpoints, impairment of tumor apoptotic pathways, repair of damaged cellular targets, and reduced drug accumulation in tumor cells (1). Among those, decreased intracellular drug accumulation is a well-studied mechanisms of cancer MDR and has been shown to result in part from tumor cell expression of the ATP-dependent drug efflux transporter P-glycoprotein (P-gp, MDR1, ABCB1; refs. 2–5). P-gp belongs to the ATP-binding cassette (ABC) superfamily of active transporters found in both prokaryotes and eukaryotes, which act as energy-dependent efflux pumps for a wide variety of low molecular weight compounds and serve physiologic transport (6–13), differentiation (14, 15), and survival (16, 17) functions in nonmalignant cells. Among the human ABC superfamily, only ABCB1, ABCC1 (MRP1; ref. 18), and ABCG2 (MXR; refs. 19, 20) have to date been shown to mediate MDR, each with distinct yet overlapping efflux substrate specificities and tissue distribution patterns (21). In human malignant melanoma, a highly chemoresistant cancer (22–24), the role of ABCB1 is limited, however (25). Chemoresistance in malignant melanoma for agents currently in clinical use for this malignancy, such as dacarbazine and temozolamide (26, 27), is mediated by molecular mechanisms, such as increased cellular sulfhydryls, altered signal transduction, and increased DNA repair (28). In contrast, the mechanism of melanoma chemoresistance to other agents, such as doxorubicin, which is ineffective in clinical melanoma therapy and thus not currently used for this cancer, is less well understood and requires further investigation.

ABCB5 [subfamily B (MDR/TAP)] is a novel human ABC transporter encoded on chromosome 7p15.3 (29). ABCB5 is the third member of the human P-gp family next to its structural paralogs ABCB1 (2–5) and ABCB4 (30). Previous studies from our laboratory showed that ABCB5, like ABCB1, acts as an energy-dependent drug efflux transporter for the fluorescent probe rhodamine-123. Moreover, ABCB5 marks CD133$^+$ progenitor cells among human epidermal melanocytes (HEM) and the transporter is expressed by a subset of G3361 malignant melanoma cells (29). In physiologic progenitor cells, ABCB5 functions to maintain membrane hyperpolarization, thereby serving as a negative regulator of cell fusion of the expressing progenitor subset and, as a consequence, of culture growth and differentiation (29). Remarkably, membrane hyperpolarization is associated with the MDR phenotype of certain cancer cells, and although a potential role of the known ABCB1 as a determinant of membrane potential has been examined recently, this transporter was not found responsible in the investigated cancer types (31). We hypothesized that ABCB5, like ABCB1, functions as a drug resistance mediator in human cancer cells. We focused on examining such a potential role of ABCB5 in human malignant melanoma, because our previous results had identified the skin as the principal tissue type for ABCB5 expression (29). We furthermore focused on doxorubicin

Note: N.Y. Frank and A. Margaryan contributed equally to this work.

Requests for reprints: Markus H. Frank, Transplantation Research Center, Brigham and Women's Hospital and Children's Hospital Boston, Harvard Medical School, 75 Francis Street, Boston, MA 02115. Phone: 617-919-2993; Fax: 617-730-0129; E-mail: mfrank@rics.bwh.harvard.edu.

as a chemotherapeutic probe to examine ABCB5-mediated drug transport, because the structurally related ABCB1 transporter effluxes doxorubicin and because malignant melanoma is highly resistant to doxorubicin treatment. Our results define a novel molecular mechanism for doxorubicin resistance in human malignant melanoma. Moreover, our findings show that ABCB5 is a novel molecular marker for a distinct subset of chemoresistant, stem cell phenotype-expressing tumor cells among melanoma bulk populations, which can be specifically targeted to enhance cytotoxic efficacy.

Materials and Methods

Cell culture and isolation. The G3361 human malignant melanoma cell line was provided by Dr. Emil Frei III (Dana-Farber Cancer Institute, Boston, MA) and was cultured as described (32). HEMs isolated from the foreskins of healthy donors were purchased from Gentaur (Brussels, Belgium) and cultured in Ham's F10 medium (Clonetics, Walkersville, MD) supplemented with 10% fetal bovine serum, 6 mmol/L HEPES and 25 μg/mL bovine pituitary extract (Invitrogen, Carlsbad, CA), 10 μg/mL insulin (Sigma, St. Louis, MO), 2.8 μg/mL hydrocortisone, 2 mmol/l L-glutamine, 100 IU/mL penicillin/streptomycin (Sigma), 0.6 ng/mL basic fibroblast growth factor (Sigma), and 10 nmol/L phorbol 12-myristate 13-acetate (Sigma) as described previously (29). The analysis of these commercially available cells was exempted from institutional review board (IRB) approval. $CD133^+$ cell populations were isolated from G3361 cultures harvested by EDTA-4Na 0.2 g/L PBS treatment (Versene, 1:5,000, Invitrogen), by positive selection using anti-CD133 monoclonal antibody (mAb)–coated magnetic microbeads (Miltenyi Biotec, Auburn, CA), and by purification in MiniMACS separation columns (Miltenyi Biotec) as described (29).

RNA extraction and reverse transcription-PCR. For RNA extraction from HEM, G3361 melanoma cells, and clinical melanoma tumors, cells were lysed in TRIzol reagent (Invitrogen) followed by isopropanol precipitation and ethanol washing. Each sample was treated with 10 units RNase-free DNase I (Boehringer Mannheim, Mannheim, Germany) and incubated at 37°C for 30 minutes followed by phenol/chloroform extraction and ethanol precipitation. For the analysis of clinical melanoma samples, patient consent was obtained and the analysis was done according to a human subjects research protocol approved by the IRB of the University of Würzburg Medical School (Würzburg, Germany, protocol 31/02). RNA derived from additional human physiologic tissues and primary malignant tumors was purchased from Clontech (Palo Alto, CA), and the analysis of these commercially available samples was exempted from IRB approval. Standard cDNA synthesis reactions were done using 5 μg RNA and the SuperScript First-Strand Synthesis System for reverse transcription-PCR (RT-PCR; Invitrogen) as per manufacturer's instructions. For PCR analysis, diluted first-strand product (5 μL, ~100 ng cDNA) was added to 45 μL of a 1 × PCR mix [50 pmol of each primer, 1 × PCR PreMix C (MasterAmp PCR Optimization kits, Epicentre, Madison, WI), 2.5 units MasterAmp TAQurate DNA Polymerase Mix (Epicentre)] and denatured at 95°C for 3 minutes, cycled 35 times at 94°C for 1 minute, 58°C for 30 seconds, and 72°C for 3 minutes, and subsequently extended at 72°C for 10 minutes. The *ABCB5* gene-specific oligonucleotide primer pair 5′-AGTGGGAAGAGTACGGTAGTCCAGCTTCTG-3′ (forward) and 5′-TCACTGCACTGACTGTGCATTCAC-3′ (reverse) was used for PCR amplification of reverse-transcribed total RNA, and the cDNA PCR product containing the full-length ABCB5 open reading frame (29) was resolved on a 1% LE agarose gel and photographed. Glyceraldehyde-3-phosphate dehydrogenase primers [5′-CGACACCCACTCCTCCACCT-3′ (forward) and 5′-GAGGTCCACCACCCTGTTGC-3′ (reverse)] were used as controls to ensure RNA integrity.

Real-time quantitative reverse transcription-PCR. Total RNA was prepared from 20 of the NCI-60 cell cultures (33) maintained at the National Cancer Institute under conditions and with passage numbers as described previously (34, 35), by using the RNeasy Mini kit (Qiagen, Valencia, CA), following the manufacturer's protocol. The integrity of the RNA was assessed by denaturing agarose gel electrophoresis (visual presence of sharp 28S and 18S bands). The RNA was quantitated by spectrophotometry. Total RNA (1 μg) was incubated with DNase I and reverse transcribed with oligo(dT) with SuperScript II RT-PCR (Life Technologies, Inc., Carlsbad, CA). Reverse transcriptase product (1 μL) was amplified by primer pairs specific for ABCB5 (Genbank accession no. AY234788). Primers were designed with Primer Express software (Applied Biosystems, Foster City, CA), and *ACTB* (β-actin) was used as a normalizing control. The primers for ABCB5 (AY234788) detection were 5′-CACAAAAGGCCATTCAGGCT-3′ (forward) and 5′-GCTGAGGAATCCACCCAATCT-3′ (reverse). The primers for β-actin were 5′-CCTGGCACCCAGCACAAT-3′ and 5′-GCCGATCCACACGGAGTACT-3′. Relative gene expression was measured with the GeneAmp 7000 Sequence Detection System (Applied Biosystems). ABCB5 expression was assessed by the ratio of the expression level in the sample against mean expression in all samples.

Antibodies. The specific IgG1κ anti-ABCB5 mAb 3C2-1D12 (29) was used in the herein reported studies, and the MOPC-31C mouse isotype control mAb (PharMingen, San Diego, CA) was used as a control. ABCB1 expression was determined using the ABCB1-specific mAb Hyb-241 (12). Phycoerythrin (PE)–conjugated anti-human CD29 (clone TS2/16) and anti-human CD44 (clone IM7) mAbs were purchased from Biolegend (San Diego, CA). PE-conjugated anti-human CD49e (clone IIA1) and anti-human CD166 (clone 3A6) mAbs were from PharMingen. PE-conjugated anti-human CD105 (clone SN6) was from Serotec (Raleigh, NC). PE-conjugated anti-human CD133 (clone AC133/1) from Miltenyi Biotec. PE-conjugated isotype control mAbs were purchased from PharMingen. Unconjugated anti-human CD29 (clone TS2/16) and anti-human CD44 (clone IM7) mAbs were purchased from Biolegend. Unconjugated anti-human CD49e (clone 5H10-27) and anti-human CD166 (clone 3A6) mAbs from PharMingen. Unconjugated anti-human CD133 (clone AC133/2) from Miltenyi Biotec. Unconjugated anti-human MelanA (clone A103) from Abcam (Cambridge, MA). Unconjugated isotype control mAbs were purchased from PharMingen. FITC-conjugated goat anti-mouse immunoglobulin secondary antibody was purchased from PharMingen. Horseradish peroxidase (HRP)– and alkaline phosphatase (AP)–conjugated secondary antibodies were purchased from DAKO (Carpinteria, CA).

Flow cytometric analysis of ABCB5 expression and DNA content analysis. G3361 melanoma cells were analyzed for surface ABCB5 expression by incubation of 1×10^6 cells for 30 minutes at 4°C with anti-ABCB5 mAb or isotype control mAb (10 μg/mL) followed by counterstaining with FITC-conjugated goat anti-mouse immunoglobulin secondary antibody and single-color flow cytometry as described (29). Analysis of coexpression of ABCB5 with the CD133, CD166, CD29, CD44, CD49e, or CD105 surface markers in G3361 melanoma cells was done by dual-color flow cytometry: G3361 cells (1×10^6) were incubated for 30 minutes at 4°C with anti-ABCB5 mAb or isotype control mAb (10 μg/mL) followed by counterstaining with FITC-conjugated goat anti-mouse immunoglobulin secondary antibody as above, and cells were subsequently incubated for 30 minutes at 4°C with PE-conjugated anti-CD133, anti-CD166, anti-CD29, anti-CD44, anti-CD49e, or anti-CD105 mAbs or PE-conjugated isotype control mAbs. Washing with staining buffer was done between each step. Dual-color flow cytometry was subsequently done with acquisition of fluorescence emission at the FL1 (FITC) and FL2 (PE) spectra on a Becton Dickinson FACScan (Becton Dickinson, San Jose, CA) as described (29). In those experiments where ABCB5 surface expression and DNA content were examined concurrently, indirect ABCB5 surface staining was done immediately before propidium iodide (PI) staining as described (29) and G3361 melanoma cells (10^6) were subsequently fixed in ice-cold 65% (v/v) ethanol in PBS, washed in cold PBS, resuspended in a PI stain mixture containing 50 μg/mL PI, 0.1% Triton X-100, 0.1 mmol/L EDTA(Na)2, and 100 units/mL RNase (all purchased from Sigma), and incubated at 37°C for 30 minutes in the dark and an additional 30 minutes on ice followed by cellular DNA content determination by flow cytometry as described previously (29).

Immunohistochemistry and immunofluorescence staining. For HRP immunoenzymatic analysis of MelanA, ABCB5, CD29, CD44, CD49e, CD133, or CD166 expression, frozen melanoma sections were fixed in acetone for

10 minutes and then dried and blocked with 0.3% peroxidase for 5 minutes. Subsequently, the slides were incubated with primary mAb or control mAb diluted in TBS plus 0.5% bovine serum albumin (BSA) for 20 minutes at 37°C in a humidified chamber and with secondary HRP-conjugated antibody for 20 minutes at 37°C in a humidified chamber. The slides were subsequently developed by incubation with 3,3′-diaminobenzidine substrate (Biogenex, San Ramon, CA) for 10 minutes and then counterstained (1 minute) with hemalaun. Rinsing with TBS was done between each step. For sequential HRP/AP immunoenzymatic double staining analysis of ABCB5 and MelanA, CD133, CD49e, or CD166 coexpression, frozen sections were first stained with primary anti-MelanA, anti-CD133, anti-CD49e, or anti-CD166 mAbs followed by secondary HRP-conjugated antibody and 3,3′-diaminobenzidine development as above. Subsequently, antibodies bound during the first staining step were eluded using EnVision K1395 Double-stain Block (DAKO) according to the manufacturer's instructions, and the slides were subsequently incubated with anti-ABCB5 primary antibody diluted in TBS plus 0.5% BSA for 20 minutes at 37°C in a humidified chamber followed by incubation with AP-conjugated secondary antibody for 20 minutes at 37°C in a humidified chamber and development by incubation with K1395 Fast Red reagent (DAKO) for 30 minutes and counterstaining with hemalaun as above. Rinsing with TBS was done between each step. Slides were covered with Glycergel (DAKO) and analyzed using a Nikon Eclipse TE 300 microscope (Nikon Instruments, Melville, NY). Images were obtained using a Spot digital camera and the Spot version 3.3.2 software package (Diagnostic Instruments, Inc., Sterling Heights, MI) and were imported into Adobe Photoshop (Adobe Systems, Mountain View, CA).

For ABCB5/CD133 immunofluorescence double staining, frozen melanoma sections were fixed in acetone for 10 minutes and then dried and blocked with 0.3% peroxidase for 5 minutes. Subsequently, the slides were incubated with primary anti-ABCB5 mAb or control mAb diluted in TBS plus 0.5% BSA for 20 minutes at 37°C in a humidified chamber and then with secondary FITC-conjugated antibody for 20 minutes at 37°C in a humidified chamber. After washing, the cells were then incubated with PE-conjugated anti-CD133 mAb followed by counterstaining of nuclei with 4′,6-diamidino-2-phenylindole (Molecular Probes, Eugene, OR). Rinsing with TBS was done between each step. Fluorescence staining was analyzed by fluorescent microscopy using a Mercury-100 W fluorescent light source (Microvideo Instruments, Avon, MA) attached to a Nikon Eclipse TE 300 microscope with the use of separate filters for each fluorochrome. The images were obtained using a Spot digital camera and the Spot version 3.3.2 software package and were imported into Adobe Photoshop.

The mean percentage of cells staining positive in immunohistochemical analysis for each marker was semiquantitatively classified (−, no positivity; +, <10% positivity; ++, 10-50% positivity; +++, >50% positivity) based on cell counting in three microscopy fields (× 400 magnification) for each staining condition.

Membrane potential measurements. Membrane potential of G3361 melanoma cells was assessed by flow cytometry using the anionic $DiBaC_4$ (3) oxonol dye (Molecular Probes) as described previously (29, 31, 36). Oxonol fluorescence intensity is known to vary as a function of cellular membrane potential, with membrane depolarization resulting in increased fluorescence intensity. Briefly, cell suspensions of 1×10^6 cells/mL PBS were incubated in the absence of mAbs or with anti-ABCB5, anti-CD133, anti-ABCB1, or isotype control mAbs (50 μg/mL) for 30 minutes at 4°C followed by addition of 150 nmol/L oxonol dye. Alternatively, as a positive control for membrane depolarization, cell suspensions were incubated with KCl (150 mmol/L) for 2 minutes at 4°C before addition of oxonol dye as described (31). After an equilibration time of 2 minutes, oxonol fluorescence intensity of 5×10^4 cells per sample was measured by flow cytometry, with acquisition of fluorescence emission at the FL1 spectrum on a Becton Dickinson FACScan as described previously (29).

Doxorubicin accumulation and transport studies. In those studies where doxorubicin content was concurrently examined with ABCB5 expression, harvested human G3361 melanoma cells (1×10^6) were incubated with 1 μmol/L doxorubicin for 30 minutes at 37°C and 5% CO_2, and the cells were subsequently washed and incubated for 30 minutes at 4°C with primary isotype control mAb, anti-ABCB5 mAb, or anti-ABCB1 mAb (10 μg/mL) followed by counterstaining with FITC-conjugated goat anti-mouse immunoglobulin antibody. For longer doxorubicin exposure periods from 1 to 24 hours, G3361 melanoma cells were cultured in flat-bottomed six-well culture plates at 37°C and 5% CO_2 in a humidified incubator in the presence or absence of 1 μmol/L doxorubicin for 1, 2, 6, or 24 hours. Cells were subsequently harvested, washed, incubated for 30 minutes at 4°C with primary anti-ABCB5 mAb or isotype control mAb (10 μg/mL), and counterstained with FITC-conjugated goat anti-mouse immunoglobulin antibody as above. Analysis of doxorubicin content and ABCB5 expression was done by dual-color flow cytometry at the FL2 (doxorubicin) and FL1 (ABCB5-FITC) emission spectra on a Becton Dickinson FACScan. For analysis of the effects of the depolarizing agent KCl on doxorubicin accumulation, untreated G3361 cells or G3361 cells, incubated with 150 mmol/L KCl for 2 minutes at 4°C as above, were exposed to 1 μmol/L doxorubicin for 2 minutes at 4°C. Intracellular doxorubicin accumulation was subsequently measured by flow cytometry at the FL2 emission spectrum on a Becton Dickinson FACScan. To examine the role of ABCB5 in doxorubicin transport, human G3361 melanoma cells (1×10^6) were either incubated in the absence of mAbs or preincubated with isotype control mAb or anti-ABCB5 mAb (20 μg/mL) for 30 minutes at 4°C, subsequently washed, and then exposed to 1 μmol/L doxorubicin for 30 minutes at 37°C and 5% CO_2. Subsequently, the cells were washed and intracellular doxorubicin accumulation was measured by flow cytometry at the FL2 emission spectrum on a Becton Dickinson FACScan immediately ($t = 0$ minute) and at $t = 90$ minutes on further incubation at 37°C and 5% CO_2 to allow for doxorubicin efflux.

Chemoresistance reversal assays. G3361 melanoma cells were seeded at 10^4 cells per well in 100 μL medium in flat-bottomed 96-well culture plates (12 replicate points) and cultured in RPMI 1640 supplemented with 10% fetal bovine serum, 6 mmol/L HEPES, 2 mmol/l L-glutamine, and 100 IU/mL penicillin/streptomycin at 37°C and 5% CO_2 in a humidified incubator. Following a 24-hour incubation period to allow cell attachment, cells were preincubated for 2 hours with the anti-ABCB5 mAb 3C2-1D12 or isotype control mAb (20 μg/mL) followed by addition of doxorubicin at 0.2 to 10 μmol/L concentrations for 24 hours. The 3-(4,5-dimethylthiazol-2-yl)-2,5-diphenyltetrazolium bromide (MTT) assay for cell viability was done at times t_0 (immediately before drug addition) and t_1 (on completion of 24-hour drug exposure) by the addition of 10 μL MTT reagent per well for 2 hours at 37°C followed by the addition of 100 μL/well dye-solubilizing detergent reagent. When formazan dye crystals were completely solubilized, absorbance was measured at a wavelength of 595 nm in a spectrophotometer and the surviving cell fraction determined from t_1/t_0 absorbance ratios with blanks subtracted. The nonparametric Mann-Whitney test was used for the statistical analysis of the results, with Ps < 0.05 considered statistically significant. Results are representative of $n = 3$ independent experiments.

Quantification of apoptosis by propidium iodide staining and flow cytometry. G3361 melanoma cells were seeded at 10^4 cells per well in 3 mL standard culture medium as above in flat-bottomed six-well culture plates at 37°C and 5% CO_2 in a humidified incubator. Following a 24-hour incubation period to allow cell attachment, cells were incubated for 24 hours in the presence or absence of anti-ABCB5 mAb 3C2-1D12 or isotype control mAb (20 μg/mL). Anti-ABCB5 mAb-treated or control cultures were subsequently harvested and fixed in ice-cold 65% (v/v) ethanol in PBS, washed in cold PBS, resuspended in a PI stain mixture containing 50 μg/mL PI, 0.1% Triton X-100, 0.1 mmol/L EDTA(Na)2, and 100 units/mL RNase (all purchased from Sigma), and incubated at 37°C for 30 minutes in the dark and an additional 30 minutes on ice followed by determination of the apoptotic cell fraction containing < 2n DNA by flow cytometry (Becton Dickinson FACScan) as described previously (12). The nonparametric Mann-Whitney test was used for the statistical analysis of the results, with Ps < 0.05 considered statistically significant. Results are representative of $n = 3$ independent experiments.

Correlation analysis between *ABCB5* gene expression and drug activity. Growth inhibition data (GI_{50} values for 20 human tumor cell lines from the NCI-60 panel) were those obtained by the Developmental

Therapeutics Program (37). Values were expressed as potencies by using the negative log of the molar concentration calculated in the National Cancer Institute screen. We focused on 119 drugs for which the mechanism of action is largely understood (37). The drug data can be found online (38). Pearson correlation coefficients were calculated for assessment of ABCB5 expression-drug potency relationships. Confidence intervals and unadjusted *P*s were obtained using Efron's bootstrap resampling method, with 10,000 bootstrap samples for each gene-drug comparison as described, and the dual criteria of $P < 0.05$ and $r < -0.3$ were used to identify significant negative correlations as described previously (39).

Results

ABCB5 tissue distribution and gene expression in clinical human malignant melanomas. We have found previously a selective expression pattern of ABCB5 among physiologic and malignant human tissues, with ABCB5 expression detected in HEM and chemoresistant G3361 malignant melanoma cells but not in the MCF-7 breast cancer or SCC-25 squamous cell carcinoma cell lines or in human peripheral blood mononuclear cells (29). We examined ABCB5 mRNA expression in a broader panel of malignant tumors and physiologic human tissues. Analysis of clinical melanoma samples was done according to a human subjects research protocol approved by the IRB of the University of Würzburg Medical School (protocol 31/02). Analysis of ABCB5 expression in additional malignant tumors and physiologic tissues was done using mRNA samples commercially available from Clontech or prepared from commercially available HEM. We found ABCB5 expressed in all of seven human clinical patient-derived melanomas, including both primary tumors and metastases (Fig. 1*A*, *top*). The clinical tumor samples examined had all been

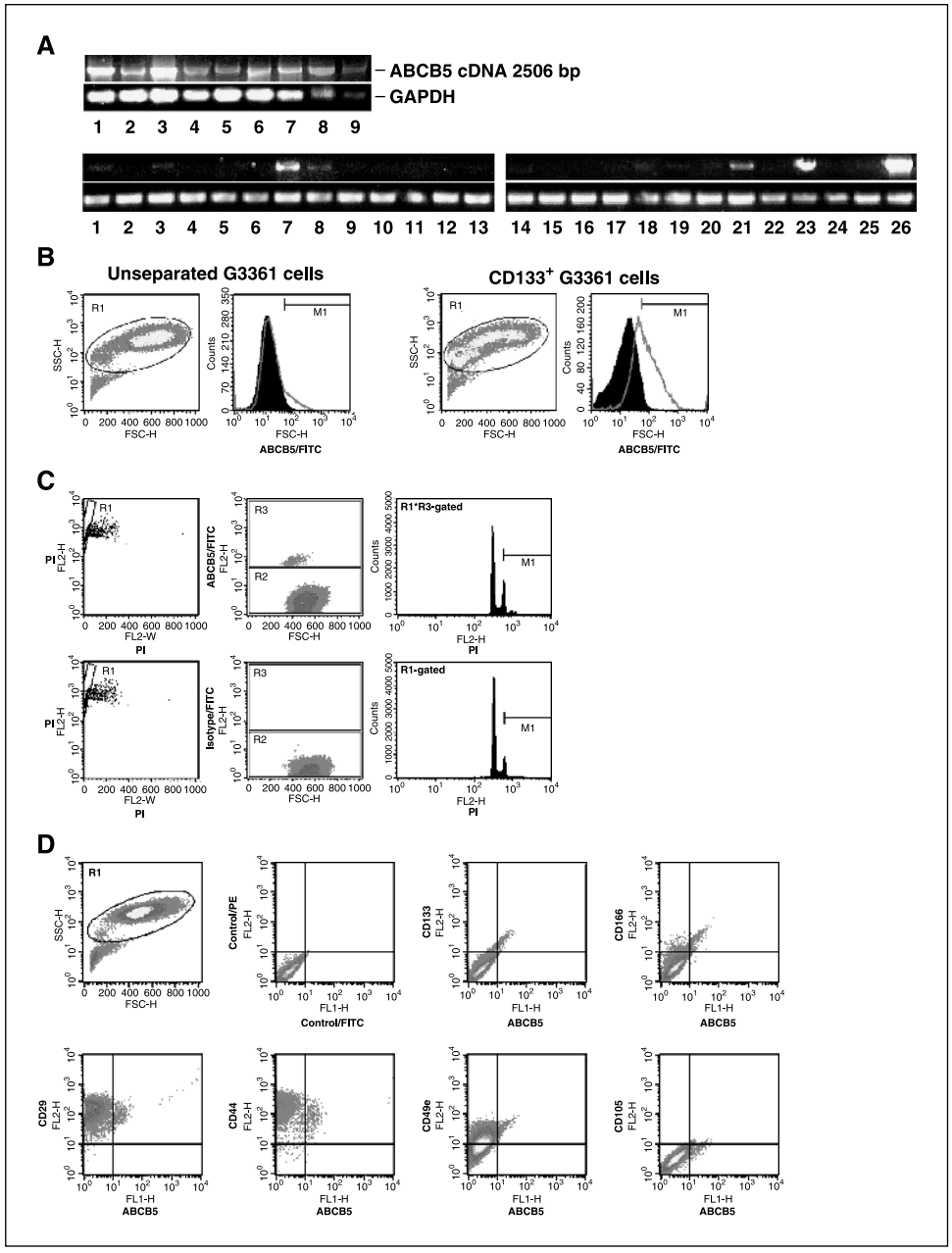

Figure 1. *ABCB5* gene expression in human malignant tumors and physiologic tissues. *A, ABCB5* gene-specific oligonucleotide primer pair [5′-AGTGG-GAAGAGTACGGTAGTCCAGCTTCTG-3′ (forward) and 5′-TCACTGCACTGACTGT-GCATTCAC-3′ (reverse)] was used for RT-PCR amplification of reverse-transcribed total RNA and the cDNA PCR product containing the full-length ABCB5 open reading frame was resolved on a 1% LE agarose gel and photographed. Glyceraldehyde-3-phosphate dehydrogenase (*GAPDH*) primers were used as controls to ensure RNA integrity. *Top, 1,* HEM; *2,* G3361 melanoma cell line; *3,* patient 1 melanoma, primary tumor; *4,* patient 2 melanoma, primary tumor; *5,* patient 3 melanoma, liver metastasis; *6,* patient 4 melanoma, lymph node metastasis; *7,* patient 5 melanoma, lymph node metastasis; *8,* patient 6 melanoma, lymph node metastasis; *9,* patient 7 melanoma, primary tumor. *Bottom, 1,* colon; *2,* fetal brain; *3,* spinal cord; *4,* salivary gland; *5,* placenta; *6,* lung; *7,* testis; *8,* stomach; *9,* prostate; *10,* uterus; *11,* kidney; *12,* trachea; *13,* small intestine; *14,* lung tumor; *15,* kidney tumor; *16,* ovary tumor; *17,* stomach tumor; *18,* colon tumor; *19,* breast tumor; *20,* thymus; *21,* breast cancer cell line; *22,* hepatoblastoma cell line; *23,* mammary gland; *24,* pancreas; *25,* adrenal gland; *26,* retina. *B,* indirect immunofluorescence staining and flow cytometry analysis of ABCB5 expression by unseparated human G3361 melanoma cells (*left*) and by purified CD133$^+$ G3361 melanoma cells (*right*). Illustrated is anti-ABCB5 mAb staining (*gray line*) and isotype control mAb staining (*shaded*). *C,* DNA content/cell cycle analysis of ABCB5$^+$ G3361 melanoma cells by dual-color flow cytometry analysis for DNA content (PI, FL2) and ABCB5 expression (FITC, FL1) using FL2-H versus FL2-W analysis (R1 gate) to exclude cell aggregates (29). *Top,* DNA content of ABCB5$^+$ cells (R1*R3-gated); *bottom,* DNA content of unseparated (R1*R2-gated) control G3361 melanoma cells. *D,* phenotypic characterization of ABCB5$^+$ human malignant melanoma cells. Dual-color flow cytometry analysis of G3361 cells costained for ABCB5 expression (FITC, FL1 fluorescence) and the CD133, CD166, CD29, CD44, CD49e, or CD105 surface markers (PE, FL2 fluorescence), respectively. ABCB5$^+$ cells coexpressing the respective surface markers are found in the *top right quadrant* of each fluorescence plot.

clinicopathologically diagnosed and classified as malignant melanomas in part based on immunohistochemical detection of MelanA (MART1) expression. The melanoma phenotype of these tumors and the relative proportion of melanoma tumor cells in the tumor specimen examined in our study were confirmed in our study by immunohistochemical analysis of MelanA expression and ABCB5/MelanA coexpression (Table 1).

Among physiologic human tissues, we found ABCB5 expressed in addition to HEM in central nervous system tissue and testis, consistent with expression of ABCB5 transcripts from these tissues reported in the Genbank database (accession nos. BM926413.1, BX453738.1, BX463401.1, and AL040762.1) and furthermore in colon, stomach, mammary gland and retina tissues (Fig. 1*A*, *bottom*). Among malignant tissues, we detected ABCB5 transcripts in addition to malignant melanoma in breast cancer cells and in a clinical breast tumor, consistent with ABCB5 expression in breast cancer reported in Genbank (accession no. BM013981.1) and furthermore in tumors from the lung, colon, and stomach (Fig. 1*A*, *bottom*). In addition, a search of the Genbank database indicates that the *ABCB5* gene is expressed in renal cell carcinoma (accession no. AI289916.1) and in malignant melanoma with high MDR (accession no. BF692596.1). Thus, ABCB5 is expressed in human skin, cultured melanoma cells, and clinical malignant melanomas. In addition, ABCB5 is expressed in select additional human physiologic and malignant tissues, including several of neuroectodermal origin.

ABCB5 expression marks melanoma cells of stem cell phenotype. Indirect surface immunostaining using anti-ABCB5 mAb and flow cytometry analysis revealed ABCB5 to be expressed on a subpopulation of G3361 melanoma cells ranging from 2% to 10% in repeat experiments (Fig. 1*B*, *left*). Further phenotypic characterization, based on the observation that ABCB5 and related ABC transporters mark physiologic progenitor cells and tumor stem cells from other tissues (29, 40–42), revealed ABCB5$^+$ cells to be specifically enriched (53% positivity) among a purified tumor cell subset of CD133$^+$ stem cell phenotype (43–46), comprising between 0.5% and 2% of all melanoma cells (Fig. 1*B*, *right*). As a corollary to our previously reported finding that ABCB5 marks polyploid progenitor cell fusion hybrids, which contribute to culture growth and differentiation in human skin (29), we examined the DNA content/cell cycle profile of ABCB5$^+$ G3361 tumor cells (Fig. 1*C*). We found that 4*n*, 6*n*, or 8*n* DNA-containing melanoma cells (M1-gated) are likewise markedly enriched among R1*R3-gated ABCB5$^+$ tumor cells (18%, *top*) compared with their frequency among whole tumor cultures (6%, *bottom*), demonstrating a distinct cell cycle profile of ABCB5$^+$ G3361 melanoma cells. ABCB5$^+$ G3361 melanoma cells nevertheless maintained a constant relative abundance vis-à-vis ABCB5$^-$ melanoma bulk population cells during long-term tumor culture expansion. Furthermore, purified CD133$^+$/ABCB5$^+$ tumor cells regenerated ABCB5-heterogenous tumor populations in culture (results not illustrated). Although the general tendency of tumor subpopulations selected for heterogeneously expressed markers to revert toward the original culture phenotype may account for these observations, these findings are also consistent with the observed stem cell phenotype of this tumor cell subpopulation among G3361 melanoma cultures, which are derived from a single tumor cell cloned in soft agar (32).

Immunofluorescence double staining confirmed coexpression of ABCB5 with the stem cell marker CD133 (AC133; refs. 43–46) on 2% of all G3361 melanoma cells (Fig. 1*D*). Further molecular phenotypic characterization directed at additional cell surface antigens known to be expressed by human malignant melanomas showed 100% positivity of ABCB5$^+$ melanoma cells for CD166 (activated leukocyte cell adhesion molecule; ref. 47), CD29 (integrin β_1; refs. 48, 49), CD49e (integrin α_5; refs. 48, 49), and CD44 (hyaluronate receptor; refs. 50, 51). CD166 and CD49e were preferentially expressed on ABCB5$^+$ tumor cells, as only 5% and 60%, respectively, of ABCB5$^-$ tumor cells expressed these markers. In contrast, CD29 and CD44 were nearly ubiquitously expressed also by ABCB5$^-$ G3361 melanoma cells (99% and 98% positivity, respectively; Fig. 1*D*). Cultured G3361 melanoma cells

Table 1. ABCB5 expression in clinical malignant melanoma

Patient	1	2	3	4	5	6
Clinicopathologic diagnosis	Malignant melanoma Clark IV	Malignant melanoma Clark IV	Malignant melanoma Clark IV	Malignant melanoma Clark IV	Malignant melanoma Clark III	Malignant melanoma Clark IV
Examined tumor specimen	Primary tumor	Metastasis liver	Metastasis lymph node	Metastasis lymph node	Metastasis lymph node	Primary tumor
ABCB5 RT-PCR	+	+	+	+	+	+
Histochemistry						
MelanA$^+$	++	+	+++	+++	+++	+++
ABCB5$^+$	+	+	++	++	++	+
MelanA$^+$/ABCB5$^+$	+	+	++	++	++	+
CD29	++	++	++	+++	+++	++
CD44	+++	+++	+++	+++	+++	+++
CD49e	++	+	++	++	++	+
CD133	++	++	++	++	++	+
CD166	+	+	++	+	++	+
Control	−	−	−	−	−	−

NOTE: Legend for immunohistochemistry: −, no positivity; +, <10% positivity; ++, 10-50% positivity; +++, >50% positivity.

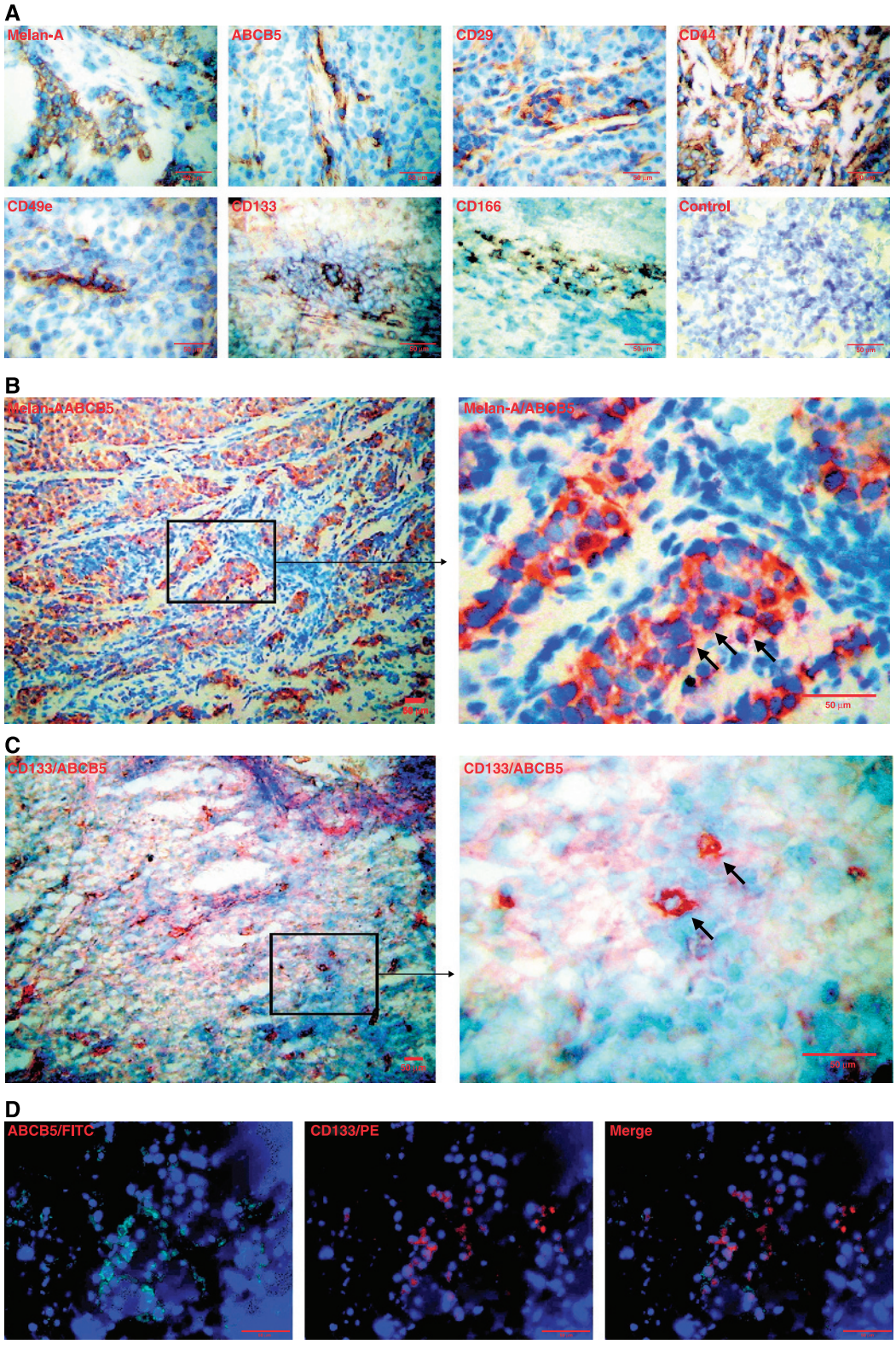

Figure 2. Immunohistochemistry and immunofluorescence analysis of ABCB5 expression in clinical human malignant melanoma sections. Representative findings from one human primary malignant melanoma (patient 7). *A,* HRP immunoenzymatic staining for MelanA, ABCB5, CD29, CD44, CD49e, CD133, or CD166 expression in frozen melanoma sections. Magnification, ×400. *B,* sequential HRP/AP immunoenzymatic double staining analysis for coexpression of MelanA (HRP, *brown*) and ABCB5 (AP, *red*). *Arrows,* representative MelanA/ABCB5 double-positive tumor cells. Magnification, ×100 (*left*) and ×400 (*right*). *C,* sequential HRP/AP immunoenzymatic double staining analysis for coexpression of CD133 (HRP, *brown*) and ABCB5 (AP, *red*). *Arrows,* representative CD133/ABCB5 double-positive tumor cells. Magnification, ×100 (*left*) and ×400 (*right*). *D,* immunofluorescence double staining of frozen melanoma sections for coexpression of ABCB5 (FITC, *green*) and CD133 (PE, *red*). Magnification, ×400. Nuclei are visualized by staining with 4′,6-diamidino-2-phenylindole (*blue*).

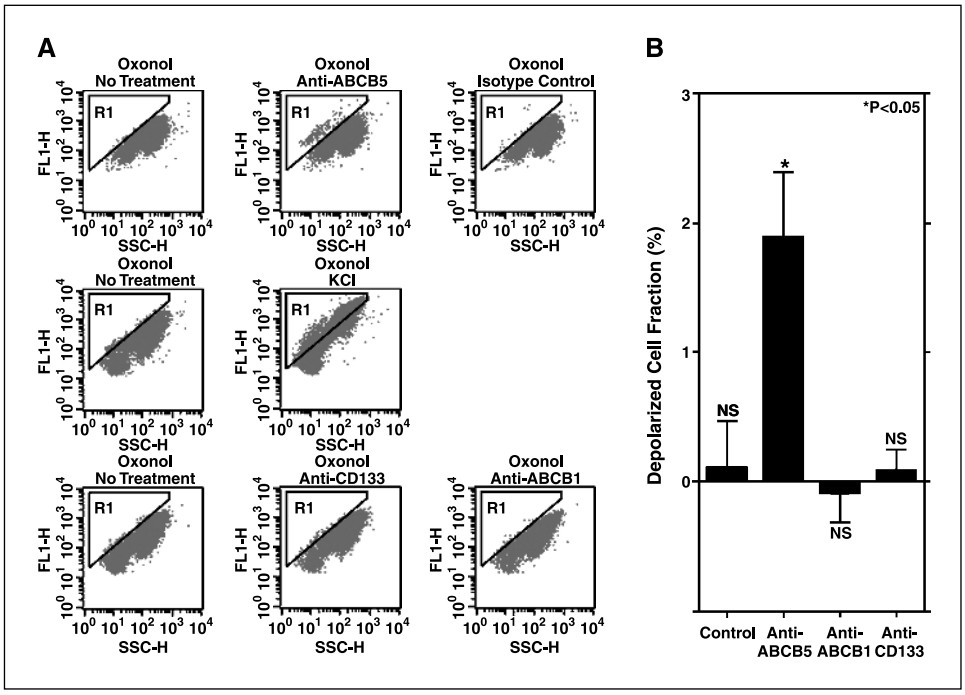

Figure 3. ABCB5-dependent regulation of membrane potential in human malignant melanoma cells. *A,* oxonol fluorescence intensity (acquired at the FL1 emission spectrum) versus SSC for untreated, ABCB5 mAb-treated, isotype control mAb-treated, KCl-treated, anti-CD133 mAb-treated, and anti-ABCB1 mAb-treated G3361 cultures. The depolarized cell fraction as a result of each treatment is shown in the R1 gate. *B,* depolarized cell fraction as a result of treatment with isotype control mAb, anti-ABCB5 mAb, anti-ABCB1 mAb, or anti-CD133 mAb versus untreated controls as a mean percentage from $n = 3$ independent experiments.

did not express significant amounts of CD105 (endoglin; ref. 52; Fig. 1*D*).

ABCB5 marks stem cell phenotype-expressing tumor cells in clinical malignant melanoma. We next examined ABCB5 protein expression in six of the seven clinical human malignant tumors in which *ABCB5* gene expression was shown and for which frozen tumor sections for immunohistochemistry and immunofluorescence analysis were available. The clinicopathologically diagnosed malignant melanoma phenotype of the examined clinical tumor specimen was confirmed by MelanA immunohistochemistry staining in all examined tumors (Fig. 2*A* and *B*; Table 1). All examined melanoma tumors (6 of 6), including both primary

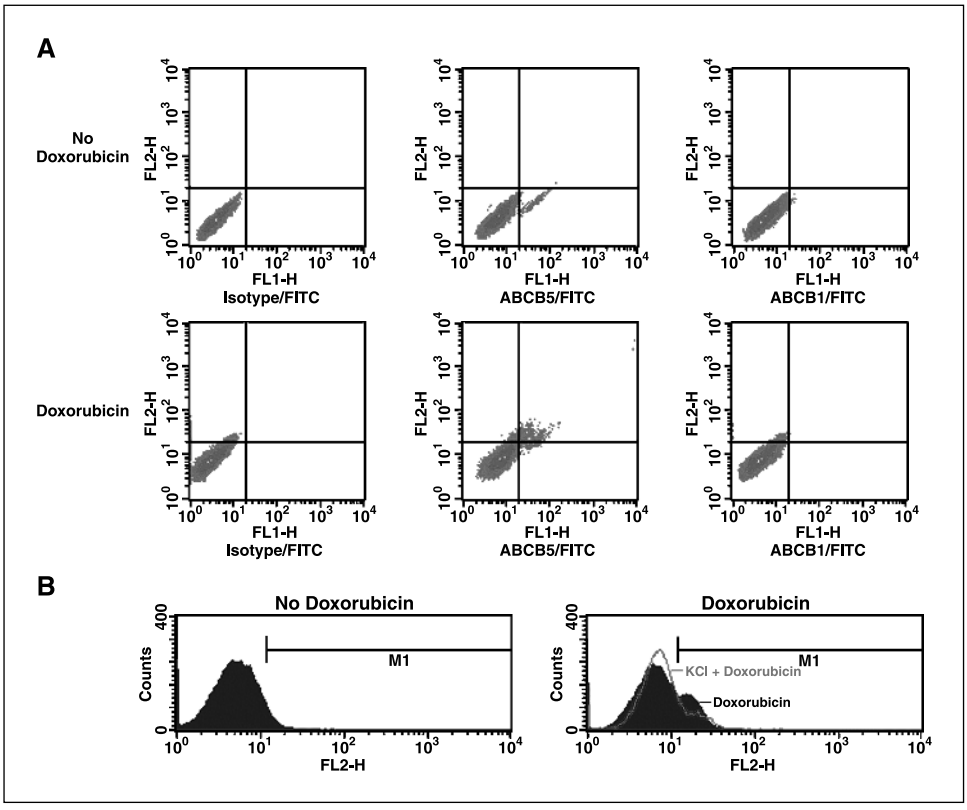

Figure 4. Differential doxorubicin content of ABCB5$^+$ melanoma cells. *A,* human G3361 melanoma cells (1×10^6) were incubated with 1 μmol/L doxorubicin for 30 minutes at 37°C and 5% CO_2. Subsequently, the cells were washed and incubated for 30 minutes at 4°C with primary isotype control mAb, anti-ABCB5 mAb, or anti-ABCB1 mAb (10 μg/mL) followed by counterstaining with FITC-conjugated goat anti-mouse immunoglobulin antibody as described (12). Analysis of doxorubicin content and cell surface marker expression was done by dual-color flow cytometry at the FL2 (doxorubicin) and FL1 (FITC) emission spectra. *Top,* no doxorubicin, *bottom,* 1 μmol/L doxorubicin. *B,* single-color flow cytometric analysis of doxorubicin content in untreated G3361 cells (*shaded*) or KCl-treated, depolarized G3361 cells (*gray line*), with doxorubicin fluorescence measured at the FL2 emission spectrum. *Left,* no doxorubicin, *right,* 1 μmol/L doxorubicin.

tumors and metastasis, also expressed ABCB5 (Fig. 2*A*; Table 1). As a corollary to our finding of ABCB5 expression on a tumor cell subpopulation in cultured human G3361 melanoma cells, we found that ABCB5 also marked a distinct tumor cell subset in clinical malignant melanomas (Fig. 2*A-D*), with <50% of cells demonstrating positivity in all tumors examined (Table 1). CD133, CD166, and CD49e similarly exhibited a restricted expression pattern, with <50% of cells demonstrating positivity, whereas CD29 and CD44 were more abundantly expressed by up to 100% of cells (Fig. 2*A*; Table 1). Immunoenzymatic costaining for ABCB5 and MelanA showed coexpression of these markers within ABCB5$^-$ MelanA$^+$ tumor cell clusters (Fig. 2*B*; Table 1) and identified ABCB5$^+$ cells as melanoma cells. We next examined ABCB5 coexpression with CD133, the stem cell marker most specifically coexpressed with ABCB5 in cultured G3361 melanoma cells, by immunoenzymatic double staining in clinical malignant melanoma. We found coexpression of ABCB5 and CD133 on select tumor cells within the clinical cancer (Fig. 2*C*). As a corollary to our finding of ABCB5 coexpression with CD166 and CD49e on cultured G3361 melanoma cells, ABCB5$^+$ cells also coexpressed CD166 and CD49e in clinical malignant melanoma as determined by immunoenzymatic double staining (results not illustrated). We also examined ABCB5 coexpression with CD133 in clinical malignant melanoma using immunofluorescence double staining as a confirmatory approach, and the results likewise showed ABCB5 and CD133 coexpression on a distinct tumor cell subpopulation within the cancer (Fig. 2*D*).

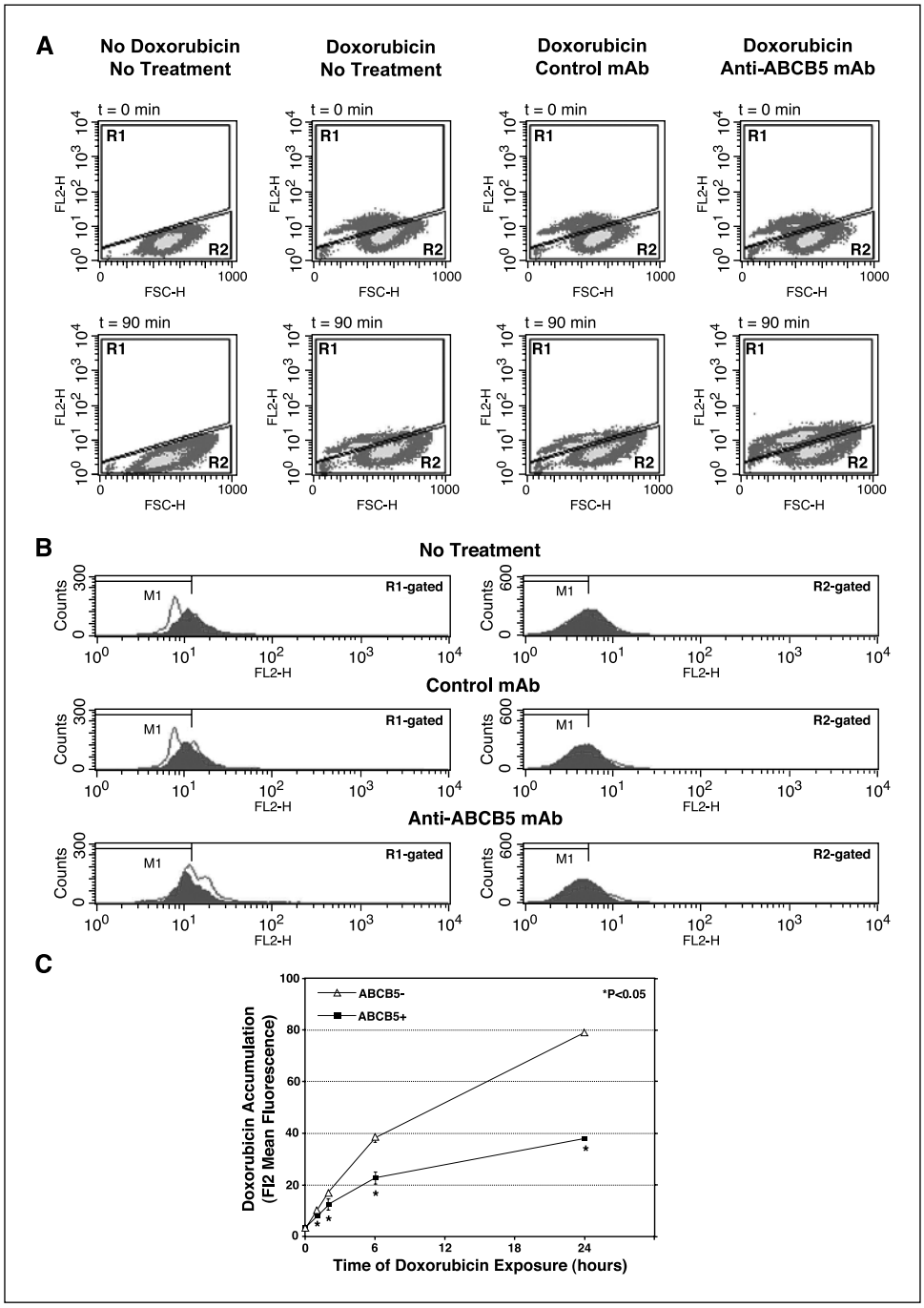

Figure 5. ABCB5 function in doxorubicin efflux transport. *A,* human G3361 melanoma cells (1×10^6) were either incubated in the absence of mAbs or preincubated with isotype control mAb or anti-ABCB5 mAb (20 μg/mL) for 30 minutes at 4°C, subsequently washed, and exposed to 1 μmol/L doxorubicin for 30 minutes at 37°C and 5% CO_2. Subsequently, the cells were washed and intracellular doxorubicin accumulation was measured by flow cytometry at the FL2 emission spectrum on a Becton Dickinson FACScan immediately (t = 0 minute, *top*) and at t = 90 minutes on further incubation at 37°C and 5% CO_2 to allow for doxorubicin efflux (*bottom*). Doxorubicin^{high} cells are shown in the R1 gate of the FL2 versus SSC plots, and doxorubicin^{low} cells are shown in the R2 gate. *B,* doxorubicin content (FL2) histogram analysis of R1-gated (*left*) or R2-gated (*right*) untreated, isotype control mAb-treated or anti-ABCB5 mAb-treated G3361 melanoma cells from Fig. 4*A* immediately on termination of doxorubicin loading (t = 0 minute, *shaded*) and 90 minutes post-doxorubicin loading (t = 90 minutes, *gray line*), with the M1 gate indicating median cellular fluorescence in untreated controls at t = 0 minute. *C,* G3361 melanoma cells were cultured in the presence 1 μmol/L doxorubicin for 1, 2, 6, or 24 hours. Cells were subsequently harvested, washed, incubated with primary anti-ABCB5 mAb or isotype control mAb, and counterstained with FITC-conjugated goat anti-mouse immunoglobulin antibody. Doxorubicin content (FL2 mean fluorescence) in ABCB5$^+$ or ABCB5$^-$ cells was determined by dual-color flow cytometry at the FL2 (doxorubicin) and FL1 (ABCB5-FITC) emission spectra on a Becton Dickinson FACScan. *Points,* mean doxorubicin content (n = 3) as a function of doxorubicin exposure time (hours); *bars,* SD.

Thus, ABCB5 identifies stem cell phenotype-expressing cancer cell subpopulations not only in cultured G3361 melanoma cells but also in clinical malignant melanoma.

ABCB5 regulates membrane potential in G3361 melanoma cells. As a corollary to our finding that ABCB5 regulates membrane potential and progenitor cell fusion in physiologic HEM, we next examined the role of ABCB5 as a determinant of plasma membrane potential in human G3361 malignant melanoma cells. Membrane potential hyperpolarization is associated with the MDR phenotype of human cancer cells (31). Using the membrane potential sensing dye oxonol, an established method to measure membrane potential (31), we found that anti-ABCB5 mAb but not isotype control mAb significantly depolarized a 1.9 ± 0.4% (mean ± SE; $P < 0.05$) low forward scatter/low side scatter (SSC) cell subset among G3361 melanoma cells compared with untreated controls (Fig. 3*A*, *top*, R1 gate, and Fig. 3*B*). Addition of the membrane depolarizing agent KCl (31) also significantly ($P < 0.05$) depolarized this cell fraction, but the effects of KCl were in addition directed at the majority of G3361 melanoma cells (86%), including ABCB5$^-$ cells (Fig. 3*A*, *middle*), consistent with a generalized effect of KCl on membrane potential. In contrast to ABCB5 blockade, neither ABCB1 blockade nor treatment with binding anti-CD133 mAb induced membrane depolarization (Fig. 3*A*, *bottom*, and Fig. 3*B*). These results show that ABCB5 functions to maintain membrane potential in the expressing tumor cell subset.

ABCB5 mediates melanoma doxorubicin resistance via its function as a doxorubicin efflux transporter. We have shown previously that ABCB5, like ABCB1, functions as a plasma membrane efflux transporter for the cationic fluorescent dye rhodamine-123 (29). We have now assessed the role of ABCB5 in cellular drug transport and chemoresistance to the cationic chemotherapeutic agent doxorubicin, also a known ABCB1 transport substrate, in ABCB5-expressing human G3361 melanoma cells. First, we found that human G3361 malignant melanoma cells are heterogeneous with regard to initial intracellular doxorubicin accumulation on incubation with 1 μmol/L doxorubicin, with a distinct subpopulation (7.2 %) of cells exhibiting high doxorubicin uptake on drug incubation (Fig. 4*A*). When ABCB5 expression and doxorubicin content were assayed concurrently, we found that 80% of ABCB5$^+$ tumor cells (9.1% of all cells) exhibited the doxorubicin^{high} phenotype, comprising the majority (59%) of doxorubicin^{high} cells (Fig. 4*A*). In contrast, neither doxorubicin^{high} nor doxorubicin^{low} G3361 melanoma cells expressed ABCB1 P-gp

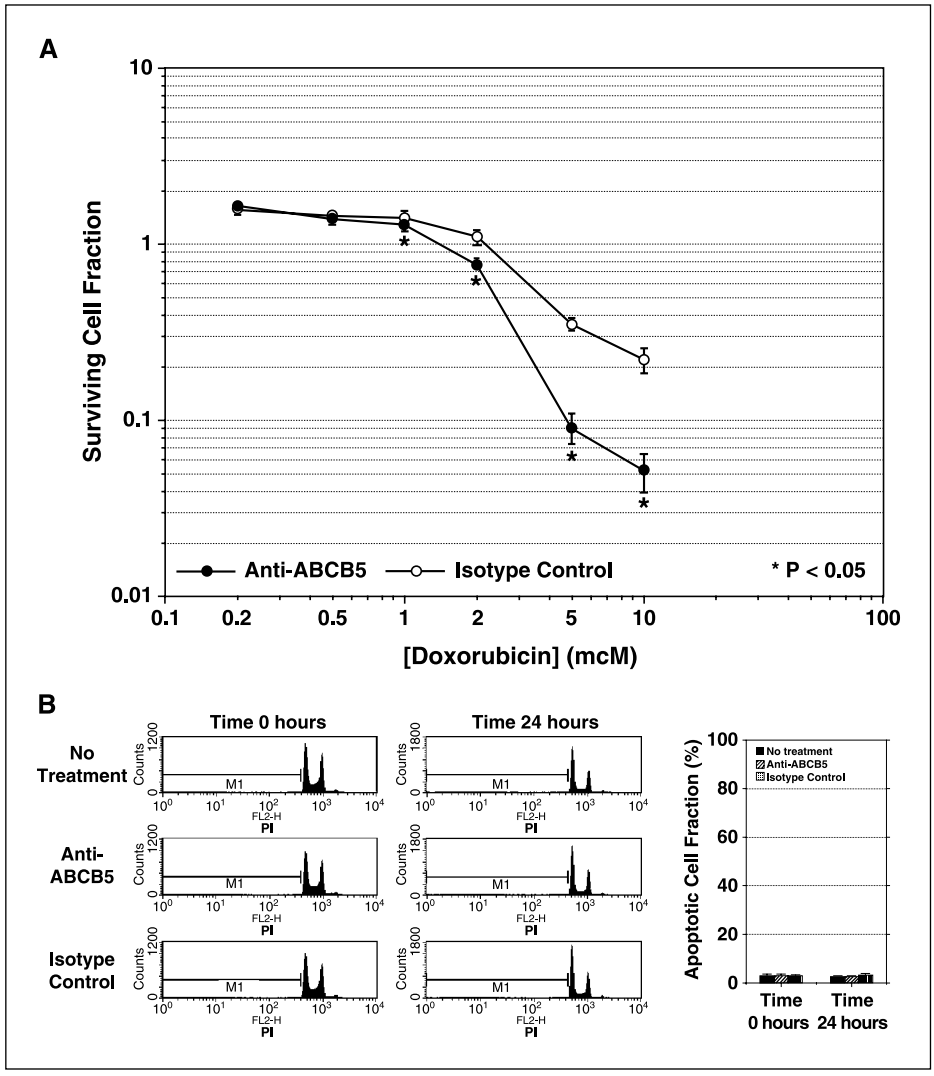

Figure 6. Melanoma doxorubicin resistance reversal by specific ABCB5 blockade. *A,* G3361 melanoma cells were seeded at 10^4 cells per well in 100 μL medium in flat-bottomed 96-well culture plates (12 replicate points) and cultured in RPMI 1640 supplemented with 10% fetal bovine serum, 6 mmol/L HEPES, 2 mmol/l L-glutamine, and 100 IU/mL penicillin/streptomycin at 37°C and 5% CO_2 in a humidified incubator. Following a 24-hour incubation period to allow cell attachment, cells were preincubated for 2 hours with the anti-ABCB5 mAb 3C2-1D12 or isotype control mAb (20 μg/mL) followed by addition of increasing concentrations of doxorubicin for 24 hours. The MTT assay for cell viability was done at times t_0 (immediately before drug addition) and t_1 (on completion of 24-hour drug exposure) by the addition of 10 μL MTT reagent per well for 2 hours at 37°C followed by the addition of 100 μL/well dye-solubilizing detergent reagent. When formazan dye crystals were completely solubilized, absorbance was measured at a wavelength of 595 nm in a spectrophotometer and the surviving cell fraction was determined from t_1/t_0 absorbance ratios with blanks subtracted. Representative of $n = 3$ independent experiments. *Points,* mean ($n = 12$) for anti-ABCB5 mAb-treated cultures (●) and isotype control mAb-treated cultures (○); *bars,* SD. *B, left,* assessment of apoptosis by PI staining of untreated, anti-ABCB5 mAb-treated, or isotype control mAb-treated G3361 cultures at times $t = 0$ and 24 hours of treatment. A leftward shift (M1 gate) in PI staining fluorescence measured at the FL2 emission spectrum indicates DNA fragmentation and cellular apoptosis. *Right, columns,* mean apoptotic cell fraction among untreated, anti-ABCB5-treated, or isotype control-treated samples ($n = 3$ independent experiments); *bars,* SD.

as determined by ABCB1-specific mAb staining (Fig. 4*A*). Importantly, anti-ABCB5 mAb treatment specifically augmented the relative frequency of doxorubicin^{high} tumor cells within samples (12.3% of all cells among anti-ABCB5 mAb-treated cultures versus 7.9% or 8.1% in isotype control mAb-treated or anti-ABCB1 mAb-treated cultures, respectively), indicating that untreated ABCB5$^+$ tumor cells not only took up doxorubicin more efficiently than ABCB5$^-$ subsets but also possessed a specific efflux capacity for doxorubicin, which was inhibited by mAb-mediated ABCB5 blockade. To address the mechanism of initial high doxorubicin uptake by ABCB5$^+$ tumor cells, we treated G3361 melanoma cells with the membrane-depolarizing agent KCl (150 mmol/L) before exposure to 1 μmol/L doxorubicin. We found that KCl significantly blocked initial high doxorubicin uptake (Fig. 4*B*, M1 gate) in 6.1 ± 0.2% (mean ± SE; $P < 0.05$) of all tumor cells, demonstrating that initial high doxorubicin uptake in this melanoma cell subpopulation is dependent on membrane hyperpolarization, a phenotype conferred by ABCB5.

To specifically show the role of ABCB5 in cellular doxorubicin efflux, we preincubated G3361 melanoma in the presence or absence of anti-ABCB5 mAb or in isotype control mAb followed by exposure to 1 μmol/L doxorubicin and subsequent analysis of intracellular doxorubicin content as a time course. We found that untreated or isotype control mAb-treated doxorubicin^{high} cells (Fig 5*A*, R1 gate of FL2 versus SSC plots), which express high levels of ABCB5, exhibited significant doxorubicin efflux over a time course of 90 minutes following completion of doxorubicin loading as evidenced by the *de novo* accumulation of 22% and 18% of doxorubicin^{high} cells (6.7% and 5.2% of all cells), respectively, in the doxorubicin efflux–measuring M1 gate (Fig. 5*B*). Untreated or isotype control mAb-treated doxorubicin^{low} cells, which do not express ABCB5 at high levels, did not significantly efflux doxorubicin (Fig. 5*A*, R2 gate of FL2 versus SSC plots). Doxorubicin efflux from doxorubicin^{high} cells (Fig. 5*A*, R1 gate of FL2 versus SSC plot) was completely inhibited by mAb-mediated ABCB5 blockade (Fig. 5*B*, M1 gate) compared with untreated or isotype control mAb-treated cultures, demonstrating the specific role of ABCB5 in cellular doxorubicin efflux transport. Moreover, when doxorubicin accumulation was assayed in cultured G3361 melanoma cells under conditions of continued drug exposure to 1 μmol/L doxorubicin in the absence of ABCB5 blockade for time periods from 1 to 24 hours, we found that ABCB5$^+$ cells accumulated significantly less doxorubicin (up to 52% reduced accumulation at 24 hours) during all exposure times tested ($P < 0.05$) compared with ABCB5$^-$ melanoma cells (Fig. 5*C*) as determined by dual-color flow cytometry for doxorubicin content (FL2 mean fluorescence) and ABCB5 expression (FITC-labeled anti-ABCB5 mAb, FL1), further supporting the demonstrated function of ABCB5 in doxorubicin efflux transport.

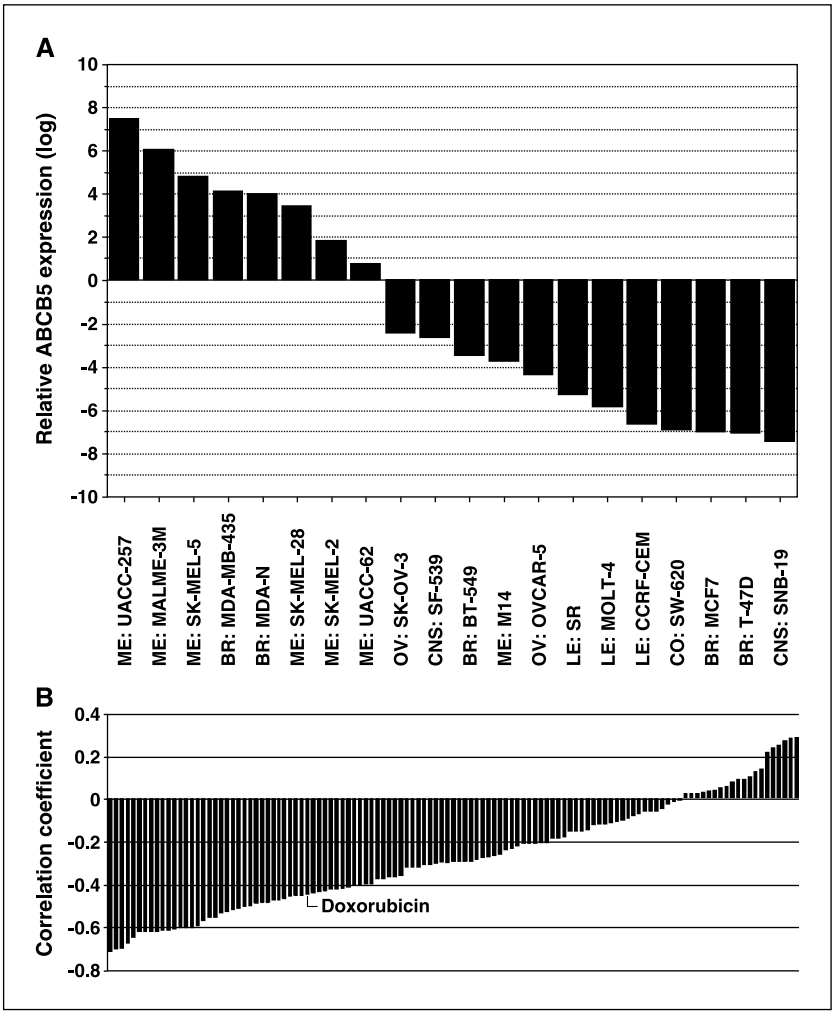

Figure 7. Correlation analysis between *ABCB5* gene expression and drug activity. *A,* relative *ABCB5* gene expression in 20 human NCI-60 cancer cell lines determined by real-time RT-PCR. *ME,* melanoma; *BR,* breast; *OV,* ovarian; *CNS,* central nervous system; *LE,* leukemia; *CO,* colon. *B,* plot of sorted correlation coefficients between *ABCB5* gene expression and cytotoxic potencies of 119 drugs. Negative values of $r < 0.3$ suggest ABCB5 transporter substrate relationships. A correlation coefficient of −0.3 is the approximate cutoff for statistical significance. The correlation coefficient between ABCB5 expression and doxorubicin ($r = -0.44$; $P = 0.016$) is indicated (see also Table 2 for additional drug correlations).

Because our results showed that ABCB5 functions as a doxorubicin efflux transporter in the ABCB5-expressing melanoma subpopulation, we next studied the role of ABCB5 in melanoma doxorubicin resistance. Clinical malignant melanoma is generally chemorefractory to the effects of doxorubicin. ABCB5 blockade by the ABCB5-specific inhibitory mAb 3C2-1D12 (29) significantly reversed the doxorubicin resistance of G3361 melanoma cells (Fig. 6), resulting in a 43% reduction in the LD_{50} from 4 to 2.3 μmol/L ($P < 0.05$) and in an additional killing of up to 26% of plated cells at 2 μmol/L (73% of control survivors killed; $P < 0.05$; Fig. 6*A*). Fractional killing of control survivors increased as a function of increasing doxorubicin concentrations, and the observed resistance reversal effect was strongest at the highest doxorubicin concentration tested (10 μmol/L; 77% of control survivors killed; $P < 0.05$), demonstrating a preferential effect of ABCB5 blockade on the chemoresistant tumor cell subset. Ninety percent cell killing (LD_{90}), not achievable in doxorubicin-treated control cells, was observed at 5 μmol/L doxorubicin (Fig. 6*A*). ABCB5 blockade alone, in the absence of doxorubicin treatment, had no significant effects on tumor cell survival and did not increase the rate of tumor cell apoptosis above the low baseline rate (<3%) observed in either untreated or isotype control mAb-treated tumor cultures (Fig. 6*B*). Thus, our results show that ABCB5 mediates melanoma doxorubicin resistance in stem cell phenotype-expressing tumor cells among heterogeneous tumor cultures by functioning as a doxorubicin efflux transporter in the expressing cell subset.

Correlation analysis between *ABCB5* gene expression and drug activity. To correlate *ABCB5* gene expression across 20 human cancer cell lines of the NCI-60 panel (33) with the growth inhibitory potencies of 119 standard anticancer drugs with known mechanisms of action, we calculated the Pearson correlation coefficient for each ABCB5-drug pair using $r < -0.3$ as a heuristic criterion for potentially significant correlations, with unadjusted bootstrap Ps < 0.05 considered statistically significant as described previously (39). *ABCB5* gene expression in the 20 human cancer cell lines determined by real-time RT-PCR is illustrated in Fig. 7*A*, with six of seven malignant melanoma cell lines demonstrating high ABCB5 expression and one of seven melanoma cell lines (M14) exhibiting low ABCB5 expression. As a corollary to our demonstration of a function of ABCB5 as a doxorubicin efflux transporter and resistance mediator, we found a significant negative correlation between ABCB5 expression and doxorubicin potency ($r = -0.44$; $P = 0.016$; Fig. 7*B*). In addition, correlation analysis between *ABCB5* gene expression and drug activity of 119 standard anticancer drugs revealed significant negative correlations for 45 of the 119 drugs considered (Fig. 7*B*; Table 2), pointing to a possible function of ABCB5 as a MDR transporter of broad specificity. These additional drug potency correlations and any underlying resistance mechanisms require likewise experimental validation as specifically shown in this study for doxorubicin (Table 2).

Discussion

We have shown previously that the novel ABCB5 member of the human P-gp family is expressed by physiologic human skin progenitor cells, regulating membrane potential and the resultant propensity for cell fusion of progenitor cells with more differentiated cell subpopulations (29). These studies also revealed that ABCB5 is expressed on a subset of chemoresistant malignant melanoma cells (29). However, whether the molecule functions as a chemotherapeutic drug efflux transporter in malignant melanoma cells and hence as a mediator of chemoresistance to specific efflux substrates, a function suggested by its close structural homology with the known human MDR transporter paralog ABCB1 P-gp, has not been investigated to date. The *ABCB5* gene encodes a family of alternatively spliced P-gp variants, of which only ABCB5 encoded by Genbank accession no. AY234788 has to date been cloned and found to function as a transporter (29). A recent correlation study of gene expression of the transportome in the NCI-60 human cancer cell lines with the potencies of 119 standard cancer drugs identified and validated the role of an alternatively spliced ABCB5 expression variant (Genbank accession no. BX453738), which does not encode a transmembrane transporter, in melanoma resistance to camptothecin, 10-OH camptothecin, and 5-fluorouracil (39), but the mechanism by which this distinct ABCB5 isoform confers chemoresistance to these agents remains elusive. In contrast, our current findings define for the first time a novel function of ABCB5 as a drug efflux transporter in human tumor cells and show an associated chemoresistance function mediated by the molecule in malignant melanoma cells for the chemotherapeutic efflux substrate doxorubicin. Consistent with these findings, expression of this full-length *ABCB5* transporter gene (encoded by Genbank accession no. AY234788) in the 20 human cancer cell lines, determined by isoform-specific real-time RT-PCR, showed significant correlation with doxorubicin resistance. Expression of the full-length isoform correlated with that of the alternatively spliced short ABCB5 variant, perhaps accounting for the correlation of the latter with anticancer drugs. Melanoma is considered refractory to the antitumor effects of doxorubicin, and this agent is therefore not currently used for melanoma therapy in the clinic. The mechanisms of clinical melanoma doxorubicin resistance are uncertain, however. Our findings provide important novel insights in this regard, indicating that ABCB5 drug efflux function may be involved. The potential relevance of ABCB5 for melanoma doxorubicin resistance is underscored by the observation that the related *ABCB1* transporter gene, which also effluxes doxorubicin (21), does not serve a significant role in human malignant melanoma (25) and is not expressed by the majority of chemoresistant human malignant melanoma cell lines (39). A potentially broader relevance of ABCB5 in cancer MDR beyond its novel role in malignant melanoma doxorubicin resistance is suggested by our detection of *ABCB5* gene expression in additional human cancers and by the significant correlation of ABCB5 expression with cancer chemoresistance to multiple agents in addition to doxorubicin. However, the role of ABCB5 in the resistance of those cancer types and in cancer resistance to additional drugs requires further functional characterization.

In elucidating the mechanism by which ABCB5 confers doxorubicin resistance, we found that $ABCB5^+$ cells exhibit lower drug accumulation than their $ABCB5^-$ counterparts under culture conditions of continuous drug exposure. In addition, ABCB5 blockade specifically enhanced doxorubicin accumulation in ABCB5-expressing tumor cells, demonstrating that ABCB5 acts as a doxorubicin efflux transporter. This function resembles that of the known structural paralog ABCB1 P-gp (21), indicating that ABCB5 and ABCB1 have overlapping substrate specificity beyond their function as efflux transporters for the fluorescent dye rhodamine-123 (29). Surprisingly, $ABCB5^+$ cells exhibited a greater initial degree of doxorubicin uptake than $ABCB5^-$ melanoma cells but, unlike $ABCB5^-$ cells, were capable of efficiently effluxing the drug, indicating that chemoresistant $ABCB5^+$ tumor cells

Table 2. Correlation between *ABCB5* gene expression and drug activity

Drug	Correlation coefficient	*P*
Camptothecin,9-NH2 (RS)	−0.7059	0.0002
Mitoxantrone	−0.6956	0.0002
Camptothecin,7-Cl	−0.6921	0.0014
Pyrazofurin	−0.6683	0.0008
Menogaril	−0.6421	0
Camptothecin,20-ester (S)	−0.6159	0.0002
Camptothecin,20-ester (S)	−0.6155	0
Camptothecin	−0.6141	0.0002
Amsacrine	−0.6118	0.0002
Etoposide	−0.6105	0.0012
Anthrapyrazole-derivative	−0.6065	0.0014
Camptothecin,20-ester (S)	−0.6038	0.0006
Teniposide	−0.6008	0
Camptothecin,11-formyl (RS)	−0.6007	0.0004
Camptothecin,10-OH	−0.5953	0.0032
Daunorubicin	−0.5879	0.0014
Camptothecin,9-NH2 (S)	−0.5672	0.0026
Deoxydoxorubicin	−0.5492	0.0006
Oxanthrazole (piroxantrone)	−0.5472	0.0042
Camptothecin,11-HOMe (RS)	−0.5280	0.0116
Zorubicin (Rubidazone)	−0.5192	0.0042
Uracil mustard	−0.5101	0.001
Camptothecin,20-ester (S)	−0.5063	0.0014
Piperazinedione	−0.5012	0.0082
Hepsulfam	−0.4920	0.0022
Melphalan	−0.4856	0.0016
Bisantrene	−0.4783	0.0136
Triethylenemelamine	−0.4755	0.0036
Spiromustine	−0.4678	0.0288
Yoshi-864	−0.4675	0.0016
Chlorambucil	−0.4594	0.002
Piperazine mustard	−0.4514	0.007
Hydroxyurea	−0.4451	0.0174
Doxorubicin	−0.4386	0.016
Porfiromycin	−0.4326	0.0158
Mechlorethamine	−0.4283	0.0348
Fluorodopan	−0.4238	0.0196
Mitomycin	−0.4173	0.0318
Cytarabine (araC)	−0.4163	0.0288
Dianhydrogalactitol	−0.4105	0.0354
Gemcitabine	−0.4088	0.0302
Thiotepa	−0.4015	0.0232
N,*N*-dibenzyl-daunomycin	−0.3940	0.0374
Teroxirone	−0.3908	0.0242
Aphidicolin-glycinate	−0.3672	0.0452

transiently accumulate higher doxorubicin concentrations than ABCB5$^-$ bulk populations. ABCB5 blockade therefore exerts its chemosensitizing effects predominantly by inducing prolonged augmented intracellular drug concentrations in this high uptake/high efflux subset via efflux inhibition. We examined the mechanism of high initial doxorubicin uptake by ABCB5$^+$ melanoma cells and found this effect to be mediated by membrane hyperpolarization, because membrane depolarization decreased early doxorubicin uptake. This finding is consistent with previous results that found intracellular doxorubicin accumulation to vary with membrane potential (53, 54). Despite increased transient doxorubicin accumulation compared with melanoma bulk populations, ABCB5$^+$ tumor cells nevertheless escaped doxorubicin-induced cell killing in the absence of ABCB5 blockade. Our demonstration of a unique cell cycle profile of ABCB5$^+$ cells suggests in this regard that additional, transport-independent mechanisms may contribute to the chemoresistance of ABCB5$^+$ tumor cells to cell cycle–specific agents. We also examined a possible antiapoptotic function of ABCB5 in this regard based on the known antiapoptotic role of ABCB1 in leukemic tumor cells (55). However, we did not find such a role for the molecule in melanoma cells, because ABCB5 blockade did not increase rates of apoptosis above controls in our experiments. Additional studies are therefore required to assess any potential contributions of ABCB5-mediated transport-independent functions to chemoresistance. Although ABCB5 blockade enhanced doxorubicin-dependent cell killing in a relatively small subset of tumor cells, the observed effect was remarkable in that it preferentially sensitized those tumor cells displaying the highest degree of doxorubicin resistance. The observed ABCB5 blockade-mediated enhancement of doxorubicin cell killing was hereby in moderate excess of the determined frequency of ABCB5$^+$ cells among untreated cultures. This finding suggests preferential growth of the chemoresistant ABCB5$^+$ cell fraction in the absence of ABCB5 blockade over the 24-hour cytotoxicity assay culture period and is consistent in magnitude with the determined growth characteristics of G3361 melanoma cells.

A further significant and novel finding of our study is the demonstration that ABCB5 is coexpressed with CD133, a marker of multipotent stem cells in human skin (46), on distinct tumor subpopulations in both cultured melanoma cells and clinical melanoma tumors, paralleling our finding that ABCB5 is preferentially expressed on CD133$^+$ stem cell phenotype-expressing subpopulations among physiologic HEM (29). Furthermore, ABCB5$^+$ tumor cells possess a DNA content profile enriched for G_2-M and polyploid 6*n* or 8*n* DNA-containing cells, resembling the cell cycle profile of HEM-associated ABCB5$^+$ progenitors (29). In addition, ABCB5$^+$ cells are hyperpolarized as a result of ABCB5 function, paralleling membrane hyperpolarization observed in physiologic skin progenitor cells (29). Thus, ABCB5$^+$ melanoma cells express a phenotype resembling that of physiologic skin-associated stem cells, raising the possibility that ABCB5 marks and mediates chemoresistance in melanoma stem cells, similar to those identified in cancers of the hematopoietic lineage by nature of their expression of different yet related MDR ABC transporters (42, 56). The existence of cancer stem cells in solid tumors has recently been proposed, and it has been suggested that tumor growth and metastasis driven by chemoresistant cancer stem cells might explain the failure of existing therapies to consistently eradicate solid tumors (57). Our study detects for the first time a distinct chemoresistant, CD133 stem cell-phenotype expressing tumor cell subset in both primary clinical melanomas and clinical melanoma metastases. ABCB5$^+$ tumor cells also preferentially express CD166, a marker implicated in melanoma metastasis (47) and associated with the physiologic stem cell phenotype (58, 59). Our findings therefore warrant further examination whether ABCB5$^+$ melanoma cells are enriched in melanoma metastases or recurrent tumors, which are thought to originate from tumor stem cells. Intriguingly, our results show that the ABCB5-expressing chemoresistant melanoma subset can be specifically targeted. This raises the possibility that ABCB5 blockade-mediated chemoresistance reversal, or novel immunotherapeutic approaches directed at ABCB5$^+$ tumor cell depletion, could potentially

enhance tumor eradication in malignant melanoma and contribute to producing more durable clinical responses than those obtained by therapeutic strategies directed predominantly at the bulk population of tumor cells.

Acknowledgments

Received 9/14/2004; revised 1/26/2005; accepted 2/25/2005.

Grant support: National Institute of Allergy and Infectious Diseases, NIH grant PO1 AI50151 (M.H. Sayegh) and KO8 AI50783 (M.H. Frank), NIH Specialized Program of Research Excellence in Skin Cancer through Brigham and Women's Hospital (M.H. Frank), Department of Defense grant BC032655 (M.H. Frank), and NIH General Medical Sciences grant GM61390 (W. Sadee).

The costs of publication of this article were defrayed in part by the payment of page charges. This article must therefore be hereby marked *advertisement* in accordance with 18 U.S.C. Section 1734 solely to indicate this fact.

We thank Dr. Emil Frei III for providing the G3361 cancer cell line used in our studies.

References

1. Gottesman MM, Fojo T, Bates SE. Multidrug resistance in cancer: role of ATP-dependent transporters. Nat Rev Cancer 2002;2:48–58.
2. Gros P, Ben Neriah YB, Croop JM, Housman DE. Isolation and expression of a complementary DNA that confers multidrug resistance. Nature 1986;323:728–31.
3. Riordan JR, Deuchars K, Kartner N, Alon N, Trent J, Ling V. Amplification of P-glycoprotein genes in multidrug-resistant mammalian cell lines. Nature 1985;316:817–9.
4. Roninson IB, Chin JE, Choi KG, et al. Isolation of human mdr DNA sequences amplified in multidrug-resistant KB carcinoma cells. Proc Natl Acad Sci U S A 1986;83:4538–42.
5. Ueda K, Cornwell MM, Gottesman MM, et al. The mdr1 gene, responsible for multidrug-resistance, codes for P-glycoprotein. Biochem Biophys Res Commun 1986;141:956–62.
6. van Helvoort A, Smith AJ, Sprong H, et al. MDR1 P-glycoprotein is a lipid translocase of broad specificity, while MDR3 P-glycoprotein specifically translocates phosphatidylcholine. Cell 1996;87:507–17.
7. Bosch I, Dunussi-Joannopoulos K, Wu RL, Furlong ST, Croop J. Phosphatidylcholine and phosphatidylethanolamine behave as substrates of the human MDR1 P-glycoprotein. Biochemistry 1997;36:5685–94.
8. Romsicki Y, Sharom FJ. Phospholipid flippase activity of the reconstituted P-glycoprotein multidrug transporter. Biochemistry 2001;40:6937–47.
9. Smit JJ, Schinkel AH, Oude Elferink RP, et al. Homozygous disruption of the murine mdr2 P-glycoprotein gene leads to a complete absence of phospholipid from bile and to liver disease. Cell 1993;75:451–62.
10. Raghu G, Park SW, Roninson IB, Mechetner EB. Monoclonal antibodies against P-glycoprotein, an MDR1 gene product, inhibit interleukin-2 release from PHA-activated lymphocytes. Exp Hematol 1996;24:1258–64.
11. Drach J, Gsur A, Hamilton G, et al. Involvement of P-glycoprotein in the transmembrane transport of interleukin-2 (IL-2), IL-4, and interferon-γ in normal human T lymphocytes. Blood 1996;88:1747–54.
12. Frank MH, Denton MD, Alexander SI, Khoury SJ, Sayegh MH, Briscoe DM. Specific MDR1 P-glycoprotein blockade inhibits human alloimmune T cell activation *in vitro*. J Immunol 2001;166:2451–9.
13. Pendse S, Sayegh MH, Frank MH. P-glycoprotein—a novel therapeutic target for immunomodulation in clinical transplantation and autoimmunity? Curr Drug Targets 2003;4:469–76.
14. Bunting KD, Galipeau J, Topham D, Benaim E, Sorrentino BP. Effects of retroviral-mediated MDR1 expression on hematopoietic stem cell self-renewal and differentiation in culture. Ann N Y Acad Sci 1999;872:125–40; discussion 140–121.
15. Randolph GJ, Beaulieu S, Lebecque S, Steinman RM, Muller WA. Differentiation of monocytes into dendritic cells in a model of transendothelial trafficking. Science 1998;282:480–3.
16. Johnstone RW, Ruefli AA, Smyth MJ. Multiple physiological functions for multidrug transporter P-glycoprotein? Trends Biochem Sci 2000;25:1–6.
17. Gollapud S, Gupta S. Anti-P-glycoprotein antibody-induced apoptosis of activated peripheral blood lymphocytes: a possible role of P-glycoprotein in lymphocyte survival. J Clin Immunol 2001;21:420–30.
18. Cole SP, Bhardwaj G, Gerlach JH, et al. Overexpression of a transporter gene in a multidrug-resistant human lung cancer cell line. Science 1992;258:1650–4.
19. Doyle LA, Yang W, Abruzzo LV, et al. A multidrug resistance transporter from human MCF-7 breast cancer cells. Proc Natl Acad Sci U S A 1998;95:15665–70.
20. Allikmets R, Schriml LM, Hutchinson A, Romano-Spica V, Dean M. A human placenta-specific ATP-binding cassette gene (ABCP) on chromosome 4q22 that is involved in multidrug resistance. Cancer Res 1998;58:5337–9.
21. Ambudkar SV, Kimchi-Sarfaty C, Sauna ZE, Gottesman MM. P-glycoprotein: from genomics to mechanism. Oncogene 2003;22:7468–85.
22. Serrone L, Hersey P. The chemoresistance of human malignant melanoma: an update. Melanoma Res 1999;9:51–8.
23. Helmbach H, Sinha P, Schadendorf D. Human melanoma: drug resistance. Recent Results Cancer Res 2003;161:93–110.
24. Li Y, McClay EF. Systemic chemotherapy for the treatment of metastatic melanoma. Semin Oncol 2002;29:413–26.
25. Goldstein LJ, Galski H, Fojo A, et al. Expression of a multidrug resistance gene in human cancers. J Natl Cancer Inst 1989;81:116–24.
26. Middleton MR, Grob JJ, Aaronson N, et al. Randomized phase III study of temozolomide versus dacarbazine in the treatment of patients with advanced metastatic malignant melanoma. J Clin Oncol 2000;18:158–66.
27. Danson S, Lorigan P, Arance A, et al. Randomized phase II study of temozolomide given every 8 hours or daily with either interferon alfa-2b or thalidomide in metastatic malignant melanoma. J Clin Oncol 2003;21:2551–7.
28. Bradbury PA, Middleton MR. DNA repair pathways in drug resistance in melanoma. Anticancer Drugs 2004;15:421–6.
29. Frank NY, Pendse SS, Lapchak PH, et al. Regulation of progenitor cell fusion by ABCB5 P-glycoprotein, a novel human ATP-binding cassette transporter. J Biol Chem 2003;278:47156–65.
30. Van der Bliek AM, Baas F, Ten Houte de Lange T, Kooiman PM, Van der Velde-Koerts T, Borst P. The human mdr3 gene encodes a novel P-glycoprotein homologue and gives rise to alternatively spliced mRNAs in liver. EMBO J 1987;6:3325–31.
31. Aleman C, Annereau JP, Liang XJ, et al. P-glycoprotein, expressed in multidrug resistant cells, is not responsible for alterations in membrane fluidity or membrane potential. Cancer Res 2003;63:3084–91.
32. Frei E III, Holden SA, Gonin R, Waxman DJ, Teicher BA. Antitumor alkylating agents: *in vitro* cross-resistance and collateral sensitivity studies. Cancer Chemother Pharmacol 1993;33:113–22.
33. Alvarez M, Paull K, Monks A, et al. Generation of a drug resistance profile by quantitation of mdr-1/P-glycoprotein in the cell lines of the National Cancer Institute Anticancer Drug Screen. J Clin Invest 1995;95:2205–14.
34. Scherf U, Ross DT, Waltham M, et al. A gene expression database for the molecular pharmacology of cancer. Nat Genet 2000;24:236–44.
35. Ross DT, Scherf U, Eisen MB, et al. Systematic variation in gene expression patterns in human cancer cell lines. Nat Genet 2000;24:227–35.
36. Grimley PM, Aszalos A. Early plasma membrane depolarization by α interferon: biologic correlation with antiproliferative signal. Biochem Biophys Res Commun 1987;146:300–6.
37. Weinstein JN, Kohn KW, Grever MR, et al. Neural computing in cancer drug development: predicting mechanism of action. Science 1992;258:447–51.
38. Weinstein JN, Myers TG, O'Connor PM, et al. An information-intensive approach to the molecular pharmacology of cancer. Science 1997;275:343–9.
39. Huang Y, Anderle P, Bussey KJ, et al. Membrane transporters and channels: role of the transportome in cancer chemosensitivity and chemoresistance. Cancer Res 2004;64:4294–301.
40. Chaudhary PM, Roninson IB. Expression and activity of P-glycoprotein, a multidrug efflux pump, in human hematopoietic stem cells. Cell 1991;66:85–94.
41. Zhou S, Schuetz JD, Bunting KD, et al. The ABC transporter Bcrp1/ABCG2 is expressed in a wide variety of stem cells and is a molecular determinant of the side-population phenotype. Nat Med 2001;7:1028–34.
42. Wulf GG, Wang RY, Kuehnle I, et al. A leukemic stem cell with intrinsic drug efflux capacity in acute myeloid leukemia. Blood 2001;98:1166–73.
43. Yin AH, Miraglia S, Zanjani ED, et al. AC133, a novel marker for human hematopoietic stem and progenitor cells. Blood 1997;90:5002–12.
44. Uchida N, Buck DW, He D, et al. Direct isolation of human central nervous system stem cells. Proc Natl Acad Sci U S A 2000;97:14720–5.
45. Schwartz PH, Bryant PJ, Fuja TJ, Su H, O'Dowd DK, Klassen H. Isolation and characterization of neural progenitor cells from post-mortem human cortex. J Neurosci Res 2003;74:838–51.
46. Belicchi M, Pisati F, Lopa R, et al. Human skin-derived stem cells migrate throughout forebrain and differentiate into astrocytes after injection into adult mouse brain. J Neurosci Res 2004;77:475–86.
47. van Kempen LC, van den Oord JJ, van Muijen GN, Weidle UH, Bloemers HP, Swart GW. Activated leukocyte cell adhesion molecule/CD166, a marker of tumor progression in primary malignant melanoma of the skin. Am J Pathol 2000;156:769–74.
48. Etoh T, Byers HR, Mihm MC Jr. Integrin expression in malignant melanoma and their role in cell attachment and migration on extracellular matrix proteins. J Dermatol 1992;19:841–6.
49. Nikkola J, Vihinen P, Vlaykova T, Hahka-Kemppinen M, Heino J, Pyrhonen S. Integrin chains β_1 and α_v as prognostic factors in human metastatic melanoma. Melanoma Res 2004;14:29–37.
50. De Wit PE, Van Muijen GN, De Waal RM, Ruiter DJ. Pathology of malignant melanoma, including new markers and techniques in diagnosis and prognosis. Curr Opin Oncol 1996;8:143–51.
51. Ahrens T, Assmann V, Fieber C, et al. CD44 is the principal mediator of hyaluronic-acid-induced melanoma cell proliferation. J Invest Dermatol 2001;116:93–101.
52. Altomonte M, Montagner R, Fonsatti E, et al. Expression and structural features of endoglin (CD105), a transforming growth factor β1 and β3 binding protein, in human melanoma. Br J Cancer 1996;74:1586–91.

53. Robinson LJ, Roepe PD. Effects of membrane potential versus pHi on the cellular retention of doxorubicin analyzed via a comparison between cystic fibrosis transmembrane conductance regulator (CFTR) and multidrug resistance (MDR) transfectants. Biochem Pharmacol 1996;52:1081–95.

54. Spalletti-Cernia D, D'Agnano I, Sorrentino R, et al. Verapamil reverts resistance to drug-induced apoptosis in Ki-ras-transformed cells by altering the cell membrane and the mitochondrial transmembrane potentials. Oncol Res 2002;13:25–35.

55. Pallis M, Turzanski J, Higashi Y, Russell N. P-glycoprotein in acute myeloid leukaemia: therapeutic implications of its association with both a multidrug-resistant and an apoptosis-resistant phenotype. Leuk Lymphoma 2002;43:1221–28.

56. Norwood K, Wang RY, Hirschmann-Jax C, et al. An *in vivo* propagated human acute myeloid leukemia expressing ABCA3. Leuk Res 2004;28:295–9.

57. Reya T, Morrison SJ, Clarke MF, Weissman IL. Stem cells, cancer, and cancer stem cells. Nature 2001;414:105–11.

58. Swart GW. Activated leukocyte cell adhesion molecule (CD166/ALCAM): developmental and mechanistic aspects of cell clustering and cell migration. Eur J Cell Biol 2002;81:313–21.

59. Oswald J, Boxberger S, Jorgensen B, et al. Mesenchymal stem cells can be differentiated into endothelial cells *in vitro*. Stem Cells 2004;22:377–84.